第 38 卷第 1 期
2019 年 2 月

红 外 与 毫 米 波 学 报
J. Infrared Millim. Waves

Vol. 38, No. 1
February, 2019

文章编号: 1001 - 9014(2019)01 - 0027 - 06

DOI: 10.11972/j.issn.1001 - 9014.2019.01.005

Fundamental W-band InP DHBT-based voltage-controlled oscillator with wide tuning range and high output power

WANG Xi[1,2], YAO Hong-Fei[1], SU Yong-Bo[1], DING Wu-Chang[1], MUHAMMAD Asif[1,2], DING Peng[1], TONG Zhi-Hang[1,2], JIN Zhi[1,2*]

(1. High-Frequency High-Voltage Device and Integrated Circuits R&D Center, Institute of Microelectronics of Chinese Academy of Sciences, Beijing 100029, China;
2. School of Electronic. Electrical and Communication Engineering, University of Chinese Academy of Sciences, Beijing 100049, China)

Abstract: A fundamental W-band voltage-controlled oscillator (VCO) featuring high output power and wide tuning range has been successfully designed. The VCO was fabricated utilizing 0.8 μm InP DHBT technology. The DHBT exhibits peak f_T of 170 GHz and f_{max} of 250 GHz. The VCO core implemented a balanced Colpitts-type topology modified for high-frequency application. An additional buffer amplifier stage was connected with the core to further boost output power as well as eliminate the load pulling effect. The DHBT base-collector P-N junction at reverse bias was chosen as a varactor diode to realize a wide frequency tuning. The measured results demonstrate that the oscillation frequency of the proposed VCO can be tuned between 81 ~ 97.3 GHz, which is a relative tuning bandwidth of 18.3 %. Over this frequency range the oscillator has a maximum output power of 10.2 dBm, and the power variation is less than 3.5 dB. A phase noise of −88 dBc/Hz@1MHz is obtained at the highest tuning frequency.

Key words: voltage-controlled oscillator, InP DHBT, wide tuning range, high output power
PACS: 84.40.Dc, 71.55.Eq, 78.55.Cr

W 波段 InP DHBT 宽带高功率压控振荡器

王 溪[1,2], 姚鸿飞[1], 苏永波[1], 丁武昌[1], 阿瑟夫[1,2], 丁 芃[1], 童志航[1,2], 金 智[1,2*]

(1. 中国科学院微电子研究所 高频高压器件与集成研发中心,北京 100029;
2. 中国科学院大学 电子电气与通信工程学院,北京 100049)

摘要: 成功实现了一款具有高输出功率和宽频率调谐范围的基波压控振荡器. 其制作工艺为 0.8 μm InP DHBT 工艺, 晶体管的最大 f_T 和 f_{max} 分别为 170 和 250 GHz. 电路核心部分采用了为高频应用改进的平衡式考毕兹拓扑,在后面添加一级缓冲放大器来抑制负载牵引效应,并提升了输出功率. DHBT 的反偏 CB 结作为变容二极管来实现频率调谐. 芯片测试结果表明,压控振荡器的频率调谐范围为 81 ~ 97.3 GHz,相对带宽为 18.3%. 在调谐频率范围内最大输出功率为 10.2 dBm,输出功率起伏在 3.5 dB 以内. 在该压控振荡器的最大调谐频率 97.3 GHz 处相位噪声为 −88 dBc/Hz @1MHz.

关 键 词: 压控振荡器; 磷化铟双异质结晶体管; 宽调谐范围; 高输出功率

中图分类号: TN431 **文献标识码:** *A*

Introduction

Millimeter-wave and sub-millimeter frequency sources are the essential part for both military and commercial applications such as communication, radar, and medical imaging systems [1]. Monolithic microwave integrated circuit (MMIC) is a good choice for these systems

Received date: 2018-04-15, **revised date:** 2018-10-21 **收稿日期:** 2018-04-15, **修回日期:** 2018-10-21
Foundation items: Supported by a key program of the National Natural Science Foundation of China (61434006)
Biography: WANG Xi (1993-), male, Shandong, Ph. D. candidate. Research area involves microwave and millimeter-wave devices and circuits. E-mail: wangxi1@ime.ac.cn
* **Corresponding author:** E-mail: jinzhi@ime.ac.cn

to achieve a frequency source with good performance and small size. Traditionally, FETs are able to deliver more power and higher frequencies of oscillations [2]. However, heterojunction bipolar transistors (HBT's) exhibit an inherently lower device flicker noise compared with high electron mobility transistors (HEMT's), and are quite popular in low phase noise VCO fabrication. InP double-HBT (DHBT) technology offers high breakdown voltage and power capabilities as well as outstanding high-frequency properties. This has been demonstrated by the reported W-band oscillators using InP HBT's and SiGe HBT's [3-4]. Meanwhile, the use of CMOS and GaN pHEMT's are also reported in W-band VCOs [5-7]. However, HBT's are better candidates for satisfying the overall requirements in frequency sources, especially in high-frequency range.

Sufficient output power is the primary requirement of high-frequency signal sources and is highly desired in some applications such as automotive radar transmitter [8]. If output power of the VCO is too low to drive next stage, the connected amplifier needs a higher gain to boost the carrier in the system. However, most of the reported VCOs have relatively low output power and narrow tuning range in W-band. The main attention here is to achieve high oscillation frequency and output power without neglecting tuning range and phase noise. In this paper, a 81 ~ 97.3 GHz (18.3% tuning range) fundamental monolithically integrated VCO is presented. Signal swing at the collector is larger, therefore, the output node is selected at the HBT collector to obtain a higher output power. Since the used InP DHBTs display a breakdown voltage BV_{ceo} greater than 6 V, a good power handling capability and signal swing could be achieved. An additional buffer amplifier stage is incorporated to further improve the power performance as well as eliminate the load pulling effect. It delivers a maximum differential output power of 10.2 dBm. The proposed MMIC VCO combines a relatively large tuning bandwidth with high output power, thus making it an appropriate frequency source in some high-frequency systems such as 94 GHz radar system.

1 InP DHBT technology

The InP DHBT technology with emitter width of 0.8 μm was used in the fabrication of the VCO. The transistor is grown on 3-inch Fe doped InP wafer with an epitaxial profile designed for high-frequency power application. The InP substrate is semi-insulating and is thinned down to 150 μm. The epitaxial layers consist of a 40 nm carbon-doped base layer and a composite collector. The 0.8* 15 μm^2 DHBT demonstrates RF figures-of-merit (f_t and f_{max}) of 170/250 GHz when biased at I_C = 15 mA and V_{CE} = 1.7 V. The device breakdown voltage BV_{ceo} could be greater than 6 V.

The InP DHBT MMIC process includes MIM capacitor, thin-film resistors (50Ω/sq), and 3-levels of metal layers (M1, M2, M3) [9]. The MIM capacitor is formed with 200 nm SiN dielectric between the capacitor metal layer and M2. Two additional interconnect layers are added with 2 μm interlayers benzocyclobutene (BCB) dielectric separating the three metal layers. Coplanar waveguide (CPW) configuration instead of microstrip is employed to achieve lower loss and eliminate the need of backside metallization and via-hole processing.

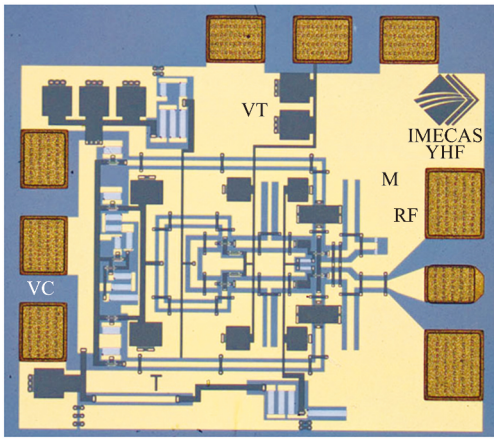

Fig. 1 Chip photo of the VCO
图1 压控振荡器芯片照片

The chip photograph is shown in Fig. 1. The total chip size is only 750 μm × 650 μm, including DC and RF probe pads.

2 Circuit design

The W-band differential VCO is implemented according to the schematic shown in Fig. 2. It consists of a VCO core based on a balanced Colpitts-type topology, extended by an output buffer amplifier.

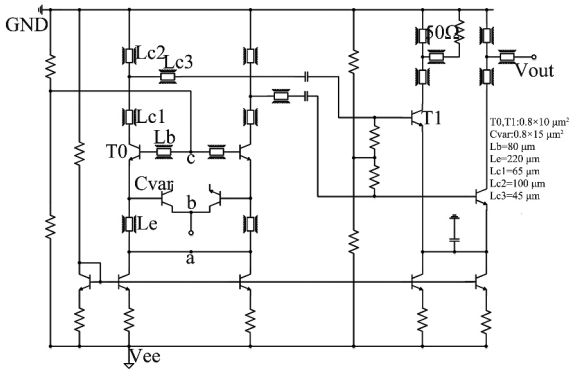

Fig. 2 Schematic circuit diagram of the balanced VCO with output buffer stage
图2 带输出缓冲级的平衡式压控振荡器原理图

The VCO core consists of two identical Colpitts configured oscillator sub-circuits, in which short coplanar transmission lines below a quarter wavelength are used as the inductively acting elements. Such a circuit configuration is selected because of its inherent negative resistance characteristic. The HBT base-collector P-N junction is used as the varactor diode C_{var}, which serves as a destabilizing element and the frequency tuning component. For the traditional VCO operating in lower frequency, the VCO resonator is formed by the capacitance C_{var} and the inductive transmission line L_b. For the W-band VCO pro-

posed in this paper, an additional short transmission line L_e is introduced to improve the performance.

Fig. 3(a) shows the simplified diagram of Colpitts oscillator and Fig. 3(b) shows the modified version for high-frequency oscillator with an additional inductor L_e. In our design the capacitor C_1 is omitted and the internal base-emitter capacitance C_{be} in the transistor takes over the role of C_1. In order to explain the effect of the added inductor L_e, we will analyze the circuits under small signal condition. The simplest transistor model- an ideal transconductance model is used here. The small signal models for the circuits in Fig. 3 are shown in Fig. 4. Analyzing Fig. 4(a) for the input impedance yields

$$Z_{in} = -\frac{g_m}{4\pi^2 f^2 C_1 C_{var}} - j\frac{1}{2\pi f}\left(\frac{1}{C_1}+\frac{1}{C_{var}}\right), \quad (1)$$

where the negative real part of Z_{in} corresponds to the negative resistance. It is obvious that the value of negative resistance is small in high-frequency. Analyzing Fig. 4(b) yields

$$Z_{in} = -\frac{g_m}{4\pi^2 f^2 C_1 C_{var} - \frac{C_1}{L_e}} - j\left(\frac{1}{2\pi f C_1}+\frac{1}{2\pi f C_{var}-\frac{1}{2\pi f L_e}}\right). \quad (2)$$

In W-band, $4\pi^2 f^2 C_1 C_{var} > 4\pi^2 f^2 C_1 C_{var} - \frac{C_1}{L_e} > 0$.

This means that by putting an additional L_e the negative resistance is boosted in higher frequency. Fig. 5 shows the simulated real part of the impedance looking into the base. As can be seen from Fig. 5, L_e help enhance negative resistance in higher frequency, making it more suitable for W-band application.

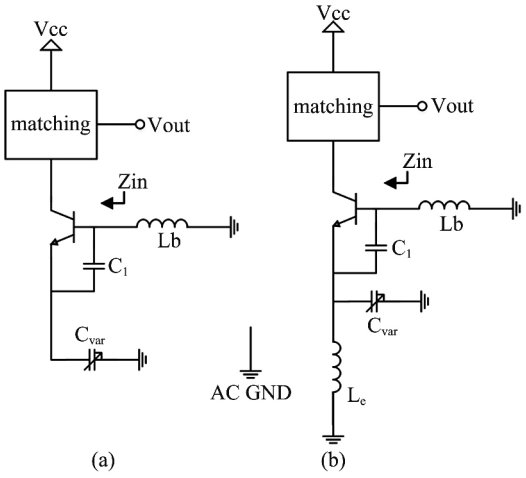

Fig. 3　(a) Simplified diagram of Colpitts oscillator (b) modified version of the Colpitts oscillator for high-frequency VCOs

图 3　(a) 考毕兹振荡器原理图 (b) 改进后适用于更高频率的考毕兹振荡器

From the simulation in Fig. 5, large negative resistance is achieved in quite a broad band, indicating that there is plenty of negative resistance margin for wideband tuning. The oscillation frequency for a Colpitts oscillator can be defined as:

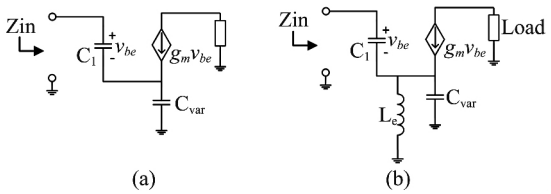

Fig. 4　Small signal models for the circuits in Fig. 3

图 4　图 3 中所示电路的小信号模型图

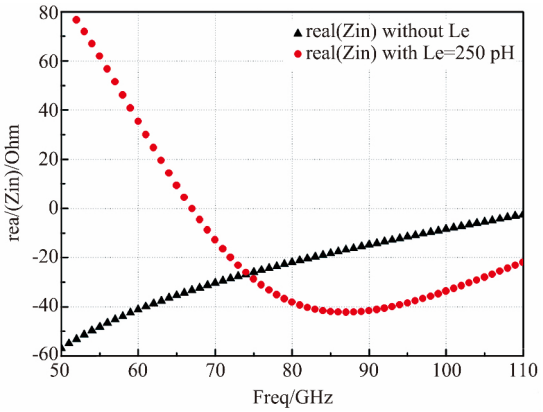

Fig. 5　Simulation results of impedance real part looking into the base with&without L_e

图 5　有无 L_e 情况下基极输入阻抗实部仿真结果

$$f_{osc} = \frac{1}{2\pi f\sqrt{L_b\frac{C_{be}C_{var}}{C_{be}+C_{var}}}}. \quad (3)$$

Large sizes for HBTs in VCO core are selected for two reasons:

(1) Transistors with large sizes allow a larger current, which enables higher output power;

(2) Transistors with large sizes have larger base-emitter capacitance (C_{be}) values. According to equation (3), a larger C_{be} leads to a wider tuning range.

The frequency tuning is obtained by changing the bias voltage of HBT base-collector P-N junction C_{var}. An excellent varactor should have larger capacitance tuning ratio and Q-factor. The lower Q-factor not only degrades phase noise performance, but also prevents oscillation at some of the tuning points, again limiting the tuning range. The selected base-collector varactor can achieve about a 2.5∶1 capacitance tuning ratio when the voltage is tuned from 0 ~ 2 V, while the capacitance value varies from 24 to 67 fF. The average value of simulated capacitance Q-factor is about 5 at the desired frequency. The capacitance tuning ratio and Q-factor prove that the base-collector diode is suitable to be used as a varactor.

In order to get a high output power, the collector of transistor T0 is used as the output as the signal swing at the collector is larger. The fabricated InP DHBT has a breakdown voltage $BV_{ceo} > 6$ V, making it suitable for high power application. For an oscillator a buffer stage is always needed to eliminate load pulling effect. The single stage common-emitter amplifier is adopted as a buffer to

maximize output power. Since the buffer amplifier could provide isolation between the load and the VCO core, it also does great help to mitigate load pulling effect [10]. The T-shaped network L_{c1}-L_{c3} serves as the inter-stage matching between the VCO core and the buffer amplifier. According to the simulation, by optimizing this inter-stage matching inductively the output power could be improved significantly. An additional T-shaped impedance matching network is applied between the buffer stage and 50 Ohm load to further boost output power at the frequency range of interest.

By using a balanced topology, virtual grounds are created for the fundamental signal at the symmetry plane such as at the points of a、b and c. In this way, the capacitance to ground can be eliminated, as ac ground can be provided at the virtual ground node. Therefore, the chip size is quite small. Mirror current sources are used to provide stable DC current to the VCO.

The circuit is simulated using the Keysight Advanced Design System (ADS). First, the small signal S-parameter analysis is used to find the oscillation frequency. Then transient analysis and harmonic balance simulation are used to ensure the oscillator performance. Finally, the EM simulation for the layout is done by the Keysight EM-simulator Momentum.

3 Measured results and discussion

The measurements of the designed W-band VCO are performed on-wafer at room temperature. The on-wafer test setup is shown in Fig. 6. An Agilent N9030A PXA signal analyzer is used for spectral measurements. The Farrantech WHMB-10-0002 75-110 GHz harmonic mixer is used to extend the frequency to W-band. The mixer has a maximum RF input power of 3 dBm and the conversion loss is 35 ~ 38 dB in this frequency range. Since the output power of the proposed VCO is greater than 3 dBm, a −10 dB attenuator is placed between the VCO and the mixer to protect the mixer from being damaged. In addition, the waveguide and the probe have about 3 dB loss in the 90 GHz band. Accordingly, the measured output power needs to be calibrated by +48 ~ 51 dB to account for the losses of probe, waveguide, attenuator and the mixer.

The VCO used a balanced topology, as this kind of topology could have two complementary outputs. When

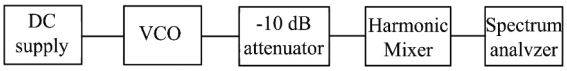

Fig. 6 On-wafer VCO test setup

图6 压控振荡器在片测试结构图

two outputs are connected with a balun which provides 180° phase shift, the fundamental frequency output power can be doubled. For measurement simplicity, we have only single-ended output in this layout design while leaving the complementary output directly connected with a 50 Ohm resistance. Theoretically, the total differential output power is 3 dB higher than the single-ended output power.

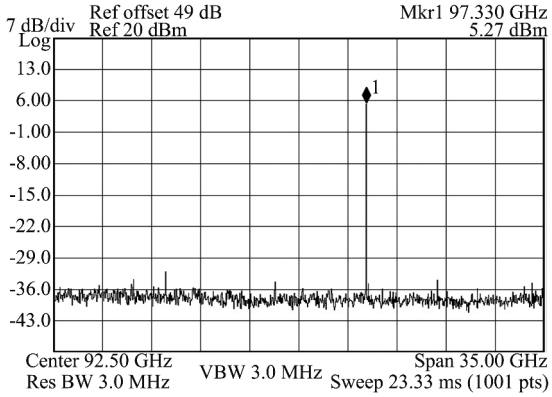

Fig. 7 The measured output spectrum of the VCO oscillating at the maximum tuning frequency

图7 压控振荡器在最大调谐频率处的输出频谱

The supply voltage V_{ee} of the VCO is −4 V with a total DC current of about 90 mA. However, the bias current mirrors consume about half of this DC power. Fig. 7 shows the measured spectrum for single-ended output at the maximum tuning frequency of 97.3 GHz. We arrive at a calibrated single-ended output power of 5.2 dBm at 97.3 GHz, corresponding to a total signal power of 8.2 dBm.

Fig. 8 (a) and (b) illustrate the measured and simulated operation frequency and the corresponding output power (P_{out}) versus the tuning voltage V_{tune}, respective-

Table 1 Comparison of some reported VCOs

表1 已报道的压控振荡器性能比较

Ref.	Process	Freq. /GHz	Tuning Range/%	P_{out}/dBm	Efficiency/%	Phase Noise/(dBc/Hz)
[4]	0.25 μm InP DHBT	113 ~ 118	4.3	−0.5	–	−89@1MHz
[11]	1.0 μm InP DHBT	88 ~ 100	12.8	7	1.4	−90@1MHz
[12]	0.5 μm InP DHBT	52.15 ~ 54.75	4.5	2.5	2.0	−89@1MHz
[13]	InP-on-BiCMOS	81.8 ~ 82.4	0.7	4.8	–	–
[6]	100 nm GaN HEMT	85.6 ~ 92.7	7.2	10.6	1.8	−87.4@1MHz
[7]	90 nm CMOS	112 ~ 117	4.4	−12	–	−93@1MHz
[8]	65 nm CMOS	96.8 ~ 108.5	11.5	–	–	−88@1MHz
This work	0.8 μm InP DHBT	81 ~ 97.3	18.3	10.2	2.9(5.8*)	−88@1MHz

P_{out} here is maximum output power.

* DC-RF efficiency after subtracting DC power consumption of mirror current source.

ly. According to Fig. 8, by varying V_{tune} the VCO can be continuously tuned from 81 GHz to 97.3 GHz. The relative tuning bandwidth is 18.3%, which is quite a wide tuning band for a W-band VCO. The maximum output power of 10.2 dBm is achieved, while the output power variation was less than 3.5 dB over this frequency range. This is a rather wide tuning frequency range as well as high output power. The high output power makes the maximum DC-RF efficiency 2.9%, and it can be 5.8% after subtracting the DC power consumption of the bias mirror current source. Compared with the measured and simulated results, both the simulated frequency and the output power are a bit larger than the measured results. This is due to the fact that the device large-signal model is not accurate enough since the model is based on 0 ~ 40 GHz measured data.

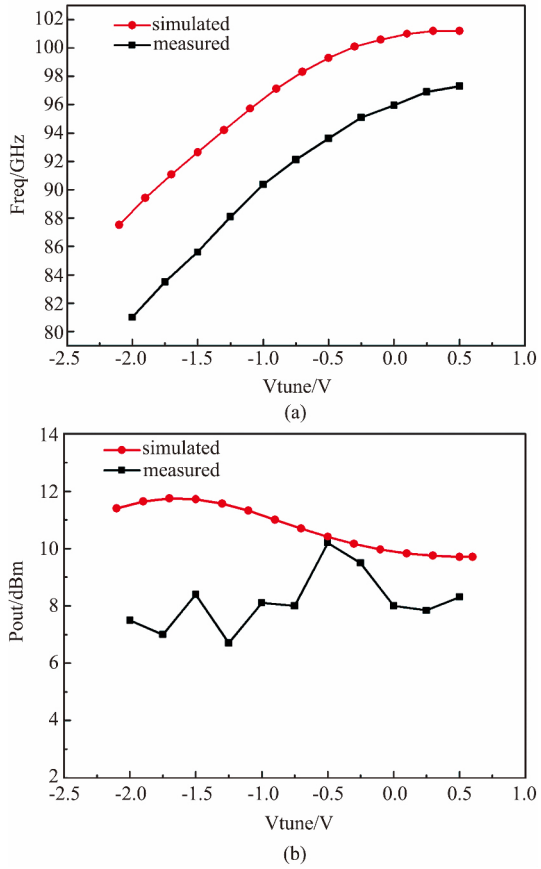

Fig. 8　(a) Measured and simulated results of the oscillation frequency as a function of the tuning voltage, (b) Measured and simulated results of the output power as a function of the tuning voltage

图 8　(a) 振荡频率测试与仿真结果对比, (b) 振荡输出功率测试与仿真结果对比

An accurate determination of phase noise is difficult in high-frequency and the noise introduced by the bias supplies complicates the measurement. Usually, a stabilization technique such as a phase locked loop will be used to minimize the phase noise of the VCO. In this case the VCO is designed as a free running oscillator. The measurement of phase noise could be estimated from the measured spectrum using the signal analyzer. A phase noise of about −88 dBc/Hz@1MHz offset was measured at the highest operation frequency of 97.3 GHz.

Among the listed results, our VCO demonstrates high output power, wide tuning bandwidth and high efficiency while the phase noise is also not bad. To the authors' knowledge, among the reported W-band InP HBT based VCOs, with such a wide tuning range this one behaves the best output power performance.

4　Conclusion

A fundamental monolithically integrated balanced VCO has been successfully designed using InP DHBT technology. By using the base-collector junction of the DHBTs as the varactor, a tuning range of 18.3% is achieved covering the frequency range in 81 ~ 97.3 GHz. The maximum single-ended output power is 7.2 dBm, resulting in a total value of 10.2 dBm. The DC power consumption is only 360 mW, among which the bias current mirrors consume about half of the DC power. The performance of this VCO in terms of frequency tuning range and output power is excellent among the published VCOs at the considered operation frequencies, and the phase noise is also good. The maximum DC-RF efficiency is 2.9%, and it could be as high as 5.8% after subtracting the DC power consumption of bias current mirrors. The total chip size is only 750 μm × 650 μm.

This work demonstrates that InP DHBT has great suitability for high performance frequency source in millimeter-wave applications.

Acknowledgments

The authors would like to thank Li Yankui for the measurement.

References

[1] Arbabian A., Callender S., Kang S., *et al*. A 94 GHz mm-wave-to-baseband pulsed-radar transceiver with applications in imaging and gesture recognition [J]. *IEEE Journal of Solid-State Circuits*, 2013, **48**(4): 1055-1071.

[2] Khanna A. P. S. State of the art in microwave VCOs [J]. *Microwave Journal*, 2015, **46**(10), 2203-2214.

[3] Rumen Kozhuharov, Mingquan Bao, Marcus Gavell, *et al*. A W- and G-band MMIC source using InP HBT technology [C]. *IEEE MTT-S International Microwave Symposium Digest*, Canada, QC, 2012: 1-3.

[4] Shinwon Kang, Jun-Chau Chien, Ali M. Niknejad. A W-Band low-noise PLL with a fundamental VCO in SiGe for millimeter-wave applications [J]. *IEEE Transaction on Microwave Theory and Techniques*, 2014, **62**(10), 2390-2404.

[5] Rainer Weber, Dirk Schwantuschke, Peter Bruckner, *et al*. A 92 GHz GaN HEMT voltage-controlled oscillator MMIC [C]. *IEEE MTT-S International Microwave Symposium*, USA, FL, 2014: 1-4.

[6] Chieh-Ying Yang, Sih-Ying Li, Sunny Cuei-Ling Hsieh, *et al*. A push-push voltage-controlled oscillator for W-band applications in 90-nm CMOS [C]. *IEEE International Symposium on Radio-Frequency Integration Technology (RFIT)*, Taiwan, Taipei, 2016: 1-3.

[7] Y. Chao, H. C. Luong, Z. Hong. Analysis and Design of a 14.1-mW 50/100-GHz Transformer-Based PLL With Embedded Phase Shifter in 65-nm CMOS [J]. *IEEE Transactions on Microwave Theory and Techniques*, 2015, **63**(4), 1193-1201.

(下转第 43 页)

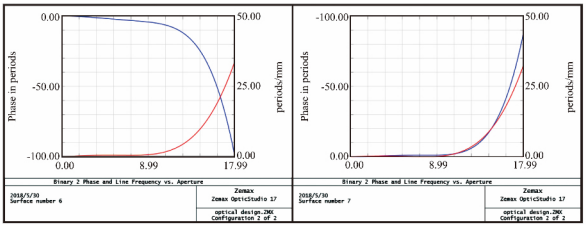

Fig. 10　Phase plot of binary surface. Left: phase plot of the optical system in the mid-infrared waveband; right: phase plot of the optical system in the far-infrared waveband

图 10　二元面在中波红外(左边)和长波红外(右边)波段的相位分布图

HDE, and the optimization method is investigated. Then an infrared telescope with a double-layer HDE is designed. Its diffraction efficiency is larger than 99% at each wavelength in the mid and far-infrared wavebands, which improves the image contrast and the image performance significantly. MTF is above 0.5 at 17 lp/mm and image performance is near-diffraction. And it is applicable to the uncooled infrared dual waveband CCD detector that has a format of 640 × 512 which's pixel pitch is 30 μm. By introducing double-layer HDE in optical design, chromatic aberration is well corrected.

References

[1] Hinnrichs M. Dual band (MWIR/LWIR) hyperspectral imager, in: 32nd [C], *Applied Imagery Pattern Recognition Workshop*, 2003, **3**: 73-78.

[2] Veldkamp W B, McHugh T J. Binary optics [J]. *Scientific American*, 1992, **266**: 92-97.

[3] Sweeney D W, Sommargren G E. Harmonic diffractive lenses [J]. *Appl Opt*, 1995, **34**: 2469-2475.

[4] Faklis D, Morris G M. Spectral properties of multiorder diffractive lenses [J]. *Appl Opt*, 1995, **34**: 2462-2468.

[5] Arieli Y. , Ozeri S. , N. Eisenberg, Design of diffractive optical elements for multiple wavelengths [J], *Opt. Lett*. 1998, **11**: 6174-6177.

[6] Chunyan, C. X. Xue, Q. F. Cui, J. B. Tong, Design of Multi-Layer Diffractive Optical Element with Bandwidth Integral Average Diffraction Efficiency [J], *Acta Optica Sinica*, 2010, **10**: 048.

[7] Sun Q, Lu Z W, Wang Z Q, The dual band design of harmonic diffractive/refractive optics system [J]. *Acta Opt. Sin*. 2004, **24**: 830-833.

[8] Sun Q, Wang Z Q. Study of an athermal infrared dual band optical system design containing harmonic diffractive element [J]. *Chin. Sci. Bull*. 2003, **48**: 1193-1198.

[9] ZHANG Liang, MAO Xin, WANG He-Long. The design of MWIR/LWIR multiple FOV optical system [J]. *J. Infrared Millim. Waves*, (**张良, 毛鑫, 王合龙. 中波/长波双色多视场光学系统设计. 红外与毫米波学报**, 2013, **32**(3): 254-259.

[10] Ma H T, Zhang X H, Han Bing. Design of telescope system with a wide spectrum, large field and small distortion [J]. *Infrared and Laser Engineering*. 2013, **7**: 020.

(上接第 31 页)

[8] Jongwon Yun, Namhyung Kim, Daekeun Yoon, *et al*. A 248-262 GHz InP HBT VCO with interesting tuning behavior [J]. *IEEE Microwave and Wireless Components Letters*, 2014, **24**(8), 560-562.

[9] Zhong Ying-Hui, Su Yong-Bo, Jin Zhi, *et al*. An InGaAs /InP W-band dynamic frequency divider [J]. *J. Infrared Millim. Waves*, (**钟英辉, 苏永波, 金智, 等. W 波段 InGaAs/InP 动态二分频器. 红外与毫米波学报**) 2012, **31**(5), 393-398.

[10] Adar A, Ramachandran R. An HBT MMIC wideband VCO [C]. *IEEE Microwave and Millimeter-wave Circuits Symposium*, USA, MA, 1991: 73-76.

[11] Makon R E, Driad R, Schneider K, *et al*. Fundamental W-Band InP DHBT-Based VCOs with low phase noise and wide tuning range [C]. *IEEE MTT-S International Microwave Symposium*, USA, HI, 2007: 649-652.

[12] Stuenkel M, Feng M. An InP VCO with static frequency divider for millimeter wave clock generation, *IEEE Compound Semiconductor Integrated Circuit Symposium* (*CSICS*), USA, CA, 2010: 1-4.

[13] Thomas Jensen, Thualfiqar Al-sawaf, Marco Lisker. Millimeter-wave hetero-integrated sources in InP-on-BiCMOS technology [J]. *International Journal of Microwave and Wireless Technologies*, 2014, **6**(3/4), 225-233.